Journal of Solid State Chemistry 182 (2009) 2852–2857

Contents lists available at ScienceDirect

Journal of Solid State Chemistry

journal homepage: www.elsevier.com/locate/jssc

Syntheses, crystal structures, and water adsorption behaviors of jungle-gym-type porous coordination polymers containing nitro moieties

Kazuhiro Uemura *, Fumiaki Onishi, Yukari Yamasaki, Hidetoshi Kita

Environmental Science and Engineering, Graduate School of Science and Engineering, Yamaguchi University, Tokiwadai 2-16-1, Ube-shi, Yamaguchi 755-8611, Japan

ARTICLE INFO

Article history:
Received 31 May 2009
Received in revised form
11 July 2009
Accepted 26 July 2009
Available online 3 August 2009

Keywords:
Zinc
Porous
Coordination polymer
Crystal structure
Adsorption
Hydrophilic

ABSTRACT

NO_2 containing dicarboxylate bridging ligands, nitroterephthalate (bdc-NO_2) and 2,5-dinitroterephthalate (bdc-$(NO_2)_2$), afford porous coordination polymers, $\{[Zn_2(bdc\text{-}NO_2)_2(dabco)]\cdot solvents\}_n$ (**2**⊃*solvents*) and $\{[Zn_2(bdc\text{-}(NO_2)_2)_2(dabco)]\cdot solvents\}_n$ (**3**⊃*solvents*). Both compounds form jungle-gym-type regularities, where a 2D square grid composed of dinuclear Zn_2 units and dicarboxylate ligands is bridged by dabco molecules to extend the 2D layers into a 3D structure. In **2**⊃*solvents* and **3**⊃*solvents*, a rectangle pore surrounded by eight Zn_2 corners contains two and four NO_2 moieties, respectively. Thermal gravimetry (TG) and X-ray powder diffraction (XRPD) measurements reveal that both compounds maintain the frameworks regularities without guest molecules and with solvents such as MeOH, EtOH, *i*-PrOH, and Me_2CO. Adsorption measurements reveal that dried **2** and **3** adsorb H_2O molecules to be $\{[Zn_2(bdc\text{-}NO_2)_2(dabco)]\cdot 4H_2O\}_n$ (**2**⊃$4H_2O$) and $\{[Zn_2(bdc\text{-}(NO_2)_2)_2(dabco)]\cdot 6H_2O\}_n$ (**3**⊃$6H_2O$), showing the pore hydrophilicity enhancement caused by NO_2 group introduction.

1. Introduction

Porous coordination polymers, namely, open metal-organic frameworks, are a new class of microporous crystalline materials and are currently receiving much attention with regard to an adsorption application [1–7]. The advantage of porous coordination polymers is that they provide an opportunity for direct pore surface engineering readily tailored by modification of the organic ligand [8], enhancing and fine-tuning the affinity for adsorbates, which is difficult for conventional porous materials such as inorganic zeolites and carbon molecular sieves. A procedure for final products of porous coordination polymers is divided into two processes: (i) framework synthesis and (ii) post-synthetic modification. A post-synthetic modification, which have recently been explored [9–14], is directly pore surface engineering, where branched functional groups inside pores are reacted with secondary added molecules to afford modified pore surfaces. On the other hand, a framework synthesis is fundamental, which has been succeeded in obtaining expected compounds by the reticular synthesis with secondary building units (SBUs) [1] or pillared layer synthesis [15]. Despite success in controlling pore size distribution by varying ligand lengths [16,17], there are some difficulties in modulating pore affinities of especially hydrophobic/hydrophilic compounds. The reason is that the rational introduction of a hydrophilic moiety into a pore is difficult due to the direct coordination of the moiety to metals.

Sometimes, porous coordination polymers are fragile and weak in humid environments, and several compounds that decompose in humid air by replacing coordinated organic ligands with H_2O were observed [18,19]. When H_2O molecules are penetrated into the pores, the interaction between H_2O molecules and hydrophilic sites (not metals) prevents frameworks from collapsing in water adsorption, therefore, the introduction of hydrogen bonding sites on the pore surfaces is effective for the stability in humid condition. On this background, we have tried to modulate $[Zn_2(bdc)_2(dabco)]_n$ (**1**, bdc = 1,4-benzenedicarboxylate and dabco = 1,4-diazabicyclo [2.2.2]octane) [20,21] by introducing protruded hydrogen bonding sites into the pores. Compound **1** has a jungle-gym-type structure [20–33], in which a 2D square grid composed of dinuclear Zn_2 units is bridged by dabco molecules to extend the 2D layers into a 3D structure, thus affording wide $7.5\times7.5\,Å^2$ open channels, which are large enough to allow the passage of small gas molecules [20]. The advantage of compound **1** is its ability to modify pore environments while maintaining the topology of the host framework [21]. Herein, selecting a nitro group as hydrogen bonding sites, we show the syntheses, crystal structures, and adsorption properties of $\{[Zn_2(bdc\text{-}NO_2)_2(dabco)]\cdot solvents\}_n$ (**2**⊃*solvents*, bdc-NO_2 = nitroterephthalate) and $\{[Zn_2(bdc\text{-}(NO_2)_2)_2(dabco)]\cdot solvents\}_n$ (**3**⊃*solvents*, bdc-$(NO_2)_2$ = 2,5-dinitroterephthalate) (Fig. 1), and discuss their stabilities in humid conditions based on H_2O adsorption measurements.

* Corresponding author at: Department of Chemistry, Faculty of Engineering, Gifu University, Yanagido 1-1, Gifu 501-1193, Japan. Fax: +81 58 293 2794.
E-mail address: k_uemura@gifu-u.ac.jp (K. Uemura).

0022-4596/$ - see front matter © 2009 Elsevier Inc. All rights reserved.
doi:10.1016/j.jssc.2009.07.048

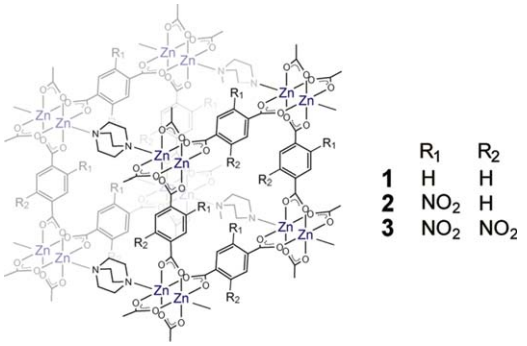

Fig. 1. Schematic view of jungle-gym-type porous coordination polymers.

2. Experimental

2.1. Materials and measurements

$Zn(NO_3)_2 \cdot 6H_2O$ was obtained from Wako Co. H_2(bdc-NO_2) and dabco were obtained from Tokyo Kasei Industrial Co. H_2(bdc-$(NO_2)_2$) was synthesized according to previous procedure [34].

Thermal gravimetry (TG) was carried out with a Rigaku Instrument TG8120 in a helium flow (100 mL/min). X-ray powder diffraction (XRPD) data were collected on a Rigaku RINT-2200YS diffractometer with Cu$K\alpha$ radiation. N_2 (77 K) adsorption measurement was carried out in Quantachrome Autsorb-1. The adsorption isotherms of gaseous H_2O were measured by using BELSORP18-Plus volumetric adsorption equipment from BEL JAPAN.

2.2. Syntheses

{[Zn_2(bdc-NO_2)$_2$(dabco)] · *solvents*}$_n$ (**2**⊃*solvents*): H_2(bdc-NO_2) (422 mg, 2.0 mmol), $Zn(NO_3)_2 \cdot 6H_2O$ (595 mg, 2.0 mmol) and dabco (112 mg, 1.0 mmol) were mixed in DMF (30 mL) and homogenized by stirring for 5 min. The slurry was heated to 120 °C in a Teflon autoclave for 48 h to obtain yellow crystals (82%). For elemental analysis and single X-ray analysis, these crystals were collected and dried in vacuo at 120 °C for 3 h to afford [Zn_2(bdc-NO_2)$_2$(dabco)]$_n$ (**2**). Elemental analysis calcd. for $C_{22}H_{18}N_4O_{12}Zn_2$ (661.18): C, 39.96; H, 2.74; N, 8.47. Found: C, 39.71; H, 2.37; N, 8.34.

{[Zn_2(bdc-$(NO_2)_2$)$_2$(dabco)] · *solvents*}$_n$ (**3**⊃*solvents*): H_2(bdc-$(NO_2)_2$) (512 mg, 2.0 mmol), $Zn(NO_3)_2 \cdot 6H_2O$ (595 mg, 2.0 mmol) and dabco (112 mg, 1.0 mmol) were mixed in DMF (60 mL) and homogenized by stirring for 5 min. The solution was heated to 120 °C in a Teflon autoclave for 48 h to obtain yellow crystals (46%). For elemental analysis, these crystals were collected and dried in vacuo at 120 °C for 6 h to afford [Zn_2(bdc-$(NO_2)_2$)$_2$(dabco)]$_n$ (**3**). Because compound **3** is moisture sensitive, elemental analysis was carried out with the sample of {[Zn_2(bdc-$(NO_2)_2$)$_2$(dabco)] · $6H_2O$}$_n$ (**3**⊃$6H_2O$). Elemental analysis calcd. for $C_{22}H_{28}N_6O_{22}Zn_2$ (859.26): C, 30.75; H, 3.28; N, 9.78. Found: C, 31.74; H, 3.16; N, 8.34.

2.3. Crystal structure determination

Single crystals of **2** and **3**⊃*solvents* were mounted on a glass fiber and coated with epoxy resin. X-ray data collections were carried out using an imaging plate detector of Rigaku RAXIS-RAPID diffractometer with graphite monochromated Mo$K\alpha$ radiation ($\lambda = 0.71075$ Å). The sizes of the unit cells were determined from reflections collected on the setting angles of three frames by changing ω by 3.0° for each frame, and intensity data were collected with a ω scan width of 5.0°. Two different χ settings were used. Empirical absorption correction [35] was performed for all data. The structures were solved by the direct method with the subsequent difference Fourier syntheses and the refinement with the SHELXTL (version 5.1) software package [36]. In **2**, the N2, O2, and O3 atoms of NO_2 moiety were isotropically refined. In **3**⊃*solvents*, obtained single crystals are too small to carry out under strict conditions. In **3**⊃*solvents*, the NO_2 moiety were found in the final state and isotropically refined under the rigid condition. The crystal data and structure refinement results are summarized in Table 1.

Table 1
Crystallographic data and structure refinements for [Zn_2(bdc-NO_2)$_2$(dabco)]$_n$ (**2**).

2	
Empirical formula	$C_{22}N_4O_{12}Zn_2$
Formula weight	643.00
Crystal system	Tetragonal
Space group	*P*4/*mmm*
a (Å)	10.9389(15)
b (Å)	10.9389(15)
c (Å)	9.6807(19)
α (deg)	90
β (deg)	90
γ (deg)	90
V (Å^3)	1158.4(3)
Z	1
Dc (Mg/m^3)	0.922
Absorption coefficient (mm^{-1})	1.074
F(000)	316
Crystal size (mm^3)	0.40 × 0.25 × 0.25
Measured reflections	11 418
Independent reflections	829 [$R_{int} = 0.0321$]
Data/restraints/parameters	829/0/51
Goodness-of fit on F^2	1.096
R [$I > 2\sigma(I)$]	$R_1 = 0.0340$, w$R_2 = 0.0921$
R (all data)	$R_1 = 0.0355$, w$R_2 = 0.0932$
Largest diff. peak and hole	0.419 and −0.364 e/Å^3

3. Results and discussion

3.1. Syntheses and thermal stabilities

Crystals of jungle-gym-type porous coordination polymer **1** are obtained by simply heating DMF solution of $Zn(NO_3)_2 \cdot 6H_2O$, bdc, and dabco with the ratio of 2:2:1 at 120 °C for 48 h [20,21]. Considering the success of replacing bdc by dicarboxylate type ligands such as 1,4-naphthalenedicarboxylate and tetrafluoroterephthalate with the maintaining jungle-gym-type regularities, a preliminary synthetic experiment using 2,5-dihydroxyterephthalic acid having hydrogen bonding sites was carried out. In that case, an expected sample was not obtained, because hydrogen bonding sites as well as carboxylic moieties can coordinate to metal as found in MOF-74 [37,38], leading to unprecedented reaction. However, selecting NO_2 moieties as the hydrogen bonding sites, isomorphous open frameworks of {[Zn_2(bdc-NO_2)$_2$(dabco)] · *solvents*}$_n$ (**2**⊃*solvents*) and {[Zn_2(bdc-$(NO_2)_2$)$_2$(dabco)] · *solvents*}$_n$ (**3**⊃*solvents*) were obtained by replacing bdc in **1** with bdc-NO_2 and bdc-$(NO_2)_2$ ligands, where the patterns of X-ray powder diffraction (XRPD) were similar to that for **1** (Fig. 2).

Fig. 3 shows the thermogram of **2**⊃*solvents* and **3**⊃*solvents* in the temperature range 20–300 °C for a heating rate $\beta = 10$ °C/min. In the temperature range 20–200 °C, the thermogram of **2**⊃*solvents* showed a mass loss (observed = 30.0%) corresponding to guest molecules. Whereas, the thermogram of **3**⊃*solvents* showed a mass

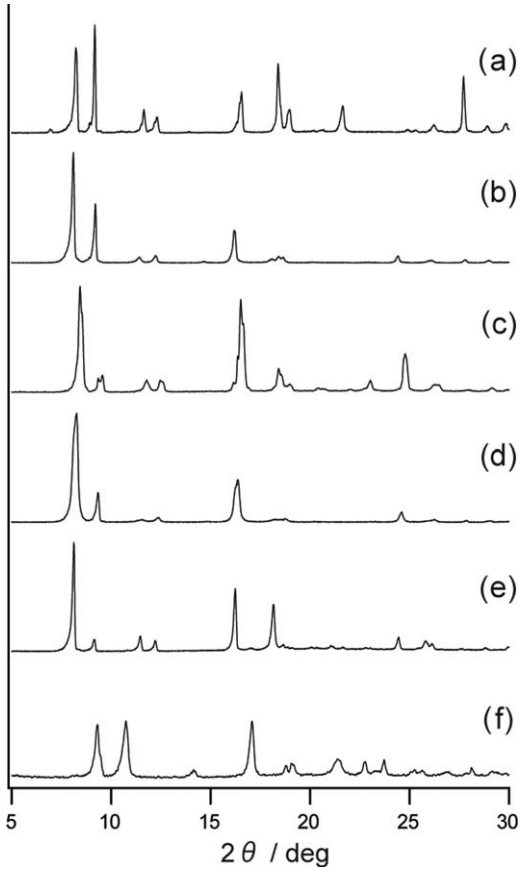

Fig. 2. XRPD patterns at room temperature for (a) $\{[Zn_2(bdc)_2(dabco)]\cdot 4DMF\cdot 1/2H_2O\}_n$ (**1**⊃4DMF·1/2H$_2$O), (b) $[Zn_2(bdc)_2(dabco)]_n$ (**1**), (c) $\{[Zn_2(bdc\text{-}NO_2)_2(dabco)]\cdot solvents\}_n$ (**2**⊃*solvents*), (d) $[Zn_2(bdc\text{-}NO_2)_2(dabco)]_n$ (**2**), (e) $\{[Zn_2(bdc\text{-}(NO_2)_2)_2(dabco)]\cdot solvents\}_n$ (**3**⊃*solvents*), and (f) $[Zn_2(bdc\text{-}(NO_2)_2)_2(dabco)]_n$ (**3**).

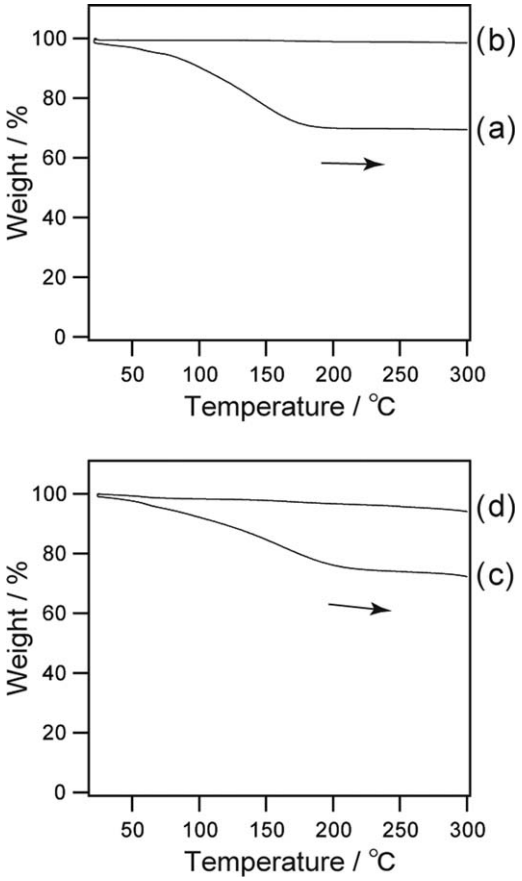

Fig. 3. TG analyses of (a) **2**⊃*solvents*, (b) drying **2**⊃*solvents* in vacuo at 120 °C for 3 h (= **2**), (c) **3**⊃*solvents*, and (d) drying **3**⊃*solvents* in vacuo at 120 °C for 6 h (= **3**), over the temperature range from 20 to 300 °C in a helium flow (100 mL/min). Heating rate: 10 °C/min.

loss (observed = 25.6%) corresponding to guest molecules in the temperature range 20–230 °C which is slightly higher temperature than that for **2**⊃*solvents*, indicating that guest molecules in **3**⊃*solvents* are more strongly bound than those in **2**⊃*solvents*. On the assumption that all guests are DMF, 3.9 and 3.5 molecules are adsorbed in one pore of **2**⊃*solvents* and **3**⊃*solvents*, respectively. Both **2**⊃*solvents* and **3**⊃*solvents* were readily de-solvated to be $[Zn_2(bdc\text{-}NO_2)_2(dabco)]_n$ (**2**) and $[Zn_2(bdc\text{-}(NO_2)_2)_2(dabco)]_n$ (**3**) by drying *in vacuo* at 120 °C for 3 and 6 h (Fig. 3b and d), respectively.

The XRPD pattern of **2** shows sharp peaks at similar peak positions of **2**⊃*solvents*, indicating that compound **2** maintains its framework after removal of the guest molecules (Fig. 2d). Similarly to the previous report [20] that the framework of $\{[Zn_2(bdc)_2(dabco)]\cdot 4DMF\cdot 1/2H_2O\}_n$ (**1**⊃4DMF·1/2H$_2$O) is expanded to be **1**, the XRPD patterns of **2** are slightly shifted to lower positions, indicating that the framework of **2** is expanded. In the case of **3**⊃*solvents*, the XRPD pattern of de-solvated **3** is different from that of **3**⊃*solvents* (Fig. 2f). In spite of the difference, indexing the reflections with a monoclinic cell by the program DICVOL91 [39] exhibits the cell parameters; monoclinic, $a = 12.639(17)$, $b = 9.375(16)$, $c = 9.564(11)$ Å, which volume ($V = 1119$ Å^3) corresponding to a rectangle surrounded by eight Zn_2 corners is similar to those of **1** and **2**. Thus, as well as **2**, dried **3** maintain their framework regularity without guest molecules.

3.2. Description of crystal structures

The structure of dried **2** was determined by single-crystal X-ray diffraction (Fig. 4). As shown in Fig. 4a and b, the bdc-NO_2 ligands that link the Zn_2 paddle-wheel units are linear, thereby forming a perfect 2D square grid linked by disordered dabco pillars. The overall 3D structure was maintained, and the bond lengths and angles around the Zn_2 paddle wheel are similar to those in compound **1** [20]. Nitro moieties are oriented to the pore with a 65.9° inclination to the benzene plane, and the dihedral angles of the benzene rings are inclined (20.0°) compared with those in **1** (Fig. 4c). As shown in Fig. 4b, there are channels along the *c*-axis with a cross-sectional area of 6.2×4.3 Å^2 [40]. In addition, single X-ray analysis for small needle crystal ($0.25 \times 0.05 \times 0.05$ mm^3) of **3**⊃*solvents* was carried out. The result reveals that **3**⊃*solvents* also form a jungle-gym-type structure, as shown in Fig. S1. Although it was difficult to obtain suitable single crystals of dried **3**, XRPD pattern exhibits the framework maintenance as mentioned in above section. Thus, both **2** and **3** form open structures without mother liquids, and are useful for the adsorption of several gases.

3.3. Adsorption properties

An N_2 (kinetic diameter: 3.64 Å) adsorption experiment was conducted at 77 K (Fig. 5). The adsorption isotherm for **2** displays a Type-I curve, corresponding to apparent BET and Langmuir surface areas of 1568 and 2000 m^2/g, respectively. In spite of bulky substitution in **2**, the surface area of **2** is comparable to that of **1** [21]. However, compound **3** hardly adsorbed N_2, and the isotherm showed a rapid rise at low relative pressure followed by a monotonically increasing curve (BET surface area: 254 m^2/g, Langmuir surface area: 258 m^2/g). These surface areas were

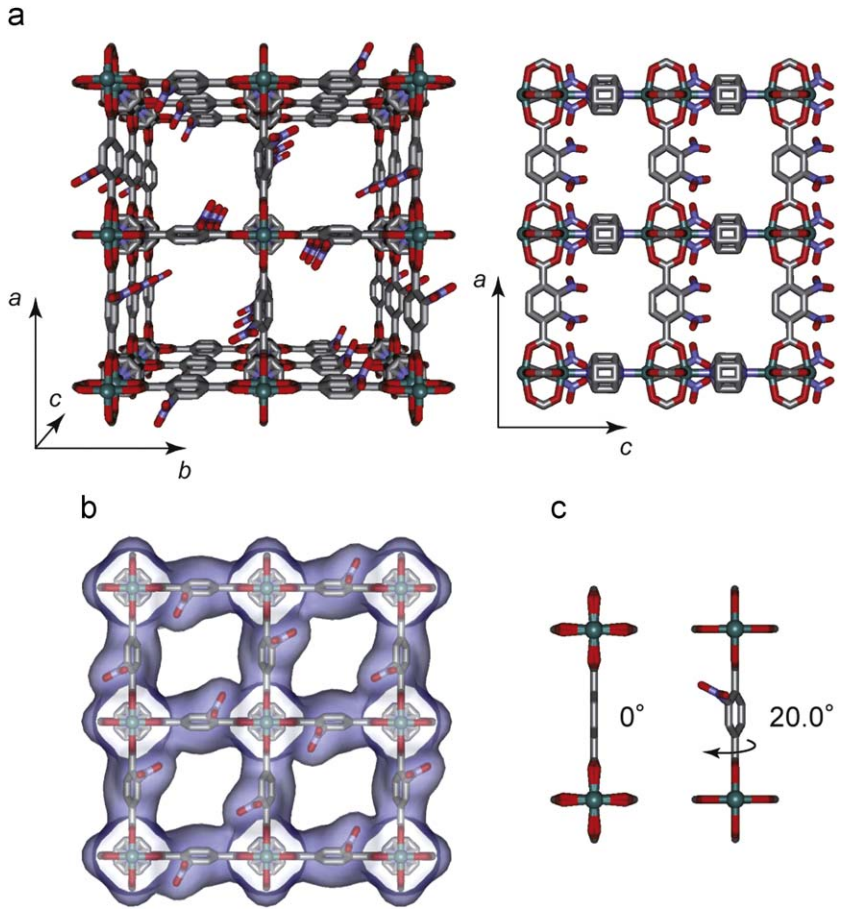

Fig. 4. (a) Crystal structures of **2** along the *c*-axis (left) and *b*-axis (right), (b) space-filling structures of **2** along the *c*-axis, and (c) inclination of the benzene rings for **1** (left) and **2** (right). Hydrogen atoms and additional nitro moieties with disorder relationship are omitted for clarity.

smaller than expected, a fact that is attributed to the small amounts of adsorption at low relative pressure, indicating no effective N_2 diffusion into the micropores. The reason would be a strong interaction of the N_2 molecules with the pore windows, which subsequently block other molecules from passing into the pore [41].

Fig. 6 shows XRPD patterns of exposed **2** to H_2O, MeOH, EtOH, *i*-PrOH, and Me_2CO. Although the relative intensities of patterns are different from that of **2** (Fig. 6d–g), the peak positions are almost coincided, indicating that the porous frameworks are maintained when **2** is exposed to organic solvents. On the other hand, H_2O exposure induces the structural transformation, because XRPD pattern is completely different from that of **2**. This structural transformation is irreversible, and H_2O molecules may be coordinated to Zn replacing bridging ligands. Fig. 7 also shows XRPD patterns of exposed **3** to H_2O, MeOH, EtOH, *i*-PrOH, and Me_2CO. The patterns of **3** exposed to organic solvents (Fig. 7d–g) have similar peak positions for as-prepared one (Fig. 7a), indicating that **3** also keeps the structure when **3** is exposed to organic solvents. This similarity supports the result that dried **3** also maintains the jungle-gym-type regularity. As being different from the case of **2**, the peak positions of **3** exposed to H_2O are almost coincided, indicating that **3** adsorbs H_2O without framework change.

Fig. 8 shows H_2O adsorption/desorption isotherms on **1**, **2** and **3** at 298 K. The isotherm of **1** shows a slight increase in low relative pressures and an abrupt rise at $P/P_0 = 0.34$ to attain the saturation of about three H_2O molecules per pore. XRPD patterns

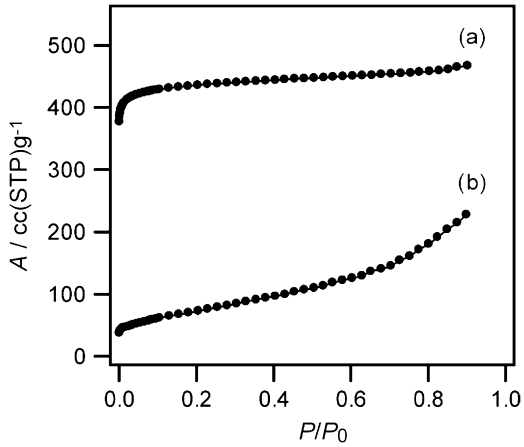

Fig. 5. Isotherm for N_2 adsorption at 77 K of (a) **2** and (b) **3**. P_0 is a saturated vapor pressure of N_2 at 77 K.

at point A [42] show new peaks that are different from the original ones, indicating the conversion to a second phase (Fig. 9, point A), whereas the adsorption isotherm of **2** shows a slight increase and steep rise after $P/P_0 = 0.3$ to assume the plateau form (four H_2O molecules per pore), like a type V isotherm. At $P/P_0 = 0.71$, the isotherm suddenly rose to attain the saturation of about six H_2O molecules per pore. Because peak positions of the XRPD patterns at point B were consistent with those of **2** (Fig. 9, point B), **2**

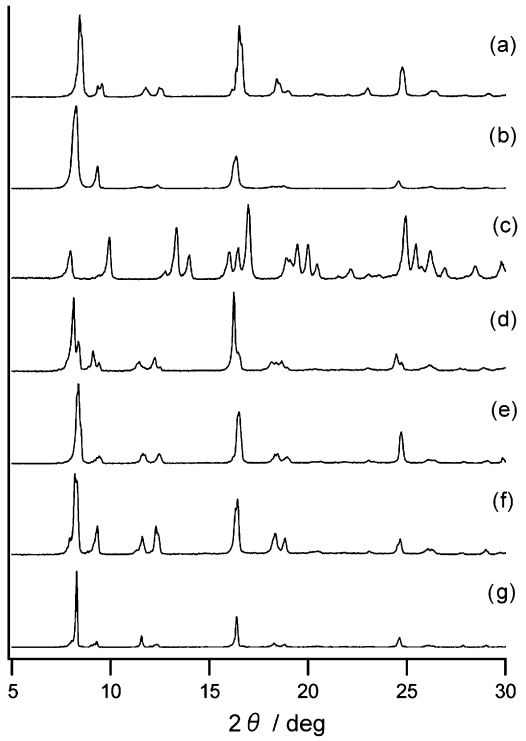

Fig. 6. XRPD patterns of (a) **2**⊃*solvents*, (b) dried **2**⊃*solvents* at 120 °C for 3 h (= **2**), exposed **2** to (c) H_2O, (d) MeOH, (e) EtOH, (f) *i*-PrOH, and (g) Me_2CO.

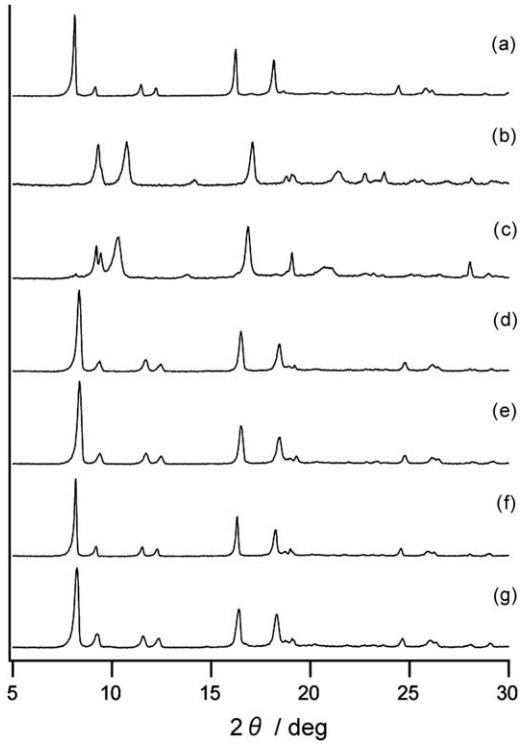

Fig. 7. XRPD patterns of (a) **3**⊃*solvents*, (b) dried **3**⊃*solvents* at 120 °C for 6 h (= **3**), exposed **3** to (c) H_2O, (d) MeOH, (e) EtOH, (f) *i*-PrOH, and (g) Me_2CO.

adsorbs H_2O to form $\{[Zn_2(bdc\text{-}NO_2)_2(dabco)]\cdot 4H_2O\}_n$ (**2**⊃$4H_2O$) keeping a jungle-gym-type structure. However, as well as **1**, **2**⊃$4H_2O$ is converted to a second phase with additional H_2O molecules (Fig. 9, point C), and the desorption isotherm does not

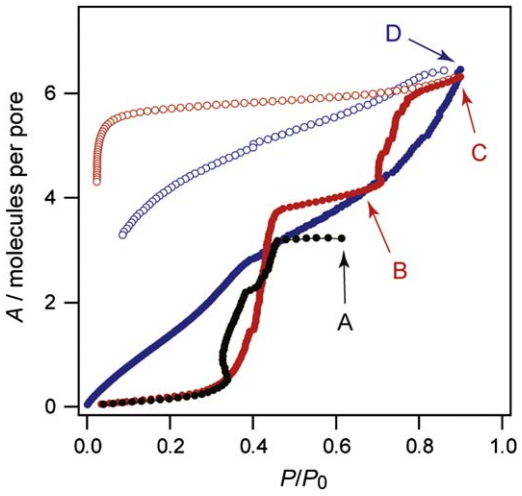

Fig. 8. Isotherms for H_2O vapor adsorption (filled circles) and desorption (open circles) on **1** (black), **2** (red), and **3** (blue) at 298 K over the relative pressure range from 0 to 0.9. P_0 is the saturated vapor pressure, 3.1690 kPa. (For interpretation of the references to color in this figure legend, the reader is referred to the web version of this article.).

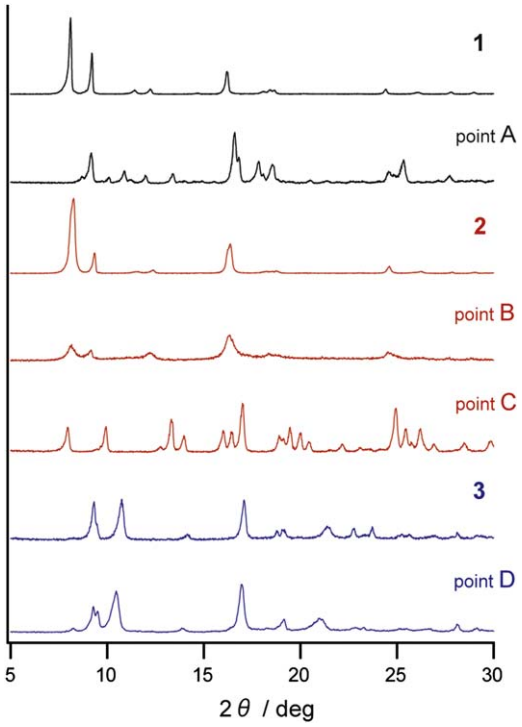

Fig. 9. XRPD patterns of **1**, **1** at point A, **2**, **2** at point B, **2** at point C, **3**, and **3** at point D. Each point is corresponding to that in Fig. 8.

retrace the adsorption isotherm. On the other hand, **3** adsorbs H_2O with a different behavior. Adsorption isotherm of **3** shows a gradual increase at low relative pressures and a monotonically increasing curve. Similar to **2** at point B, peak position of the XRPD patterns at point D are consistent with those of **3**, indicating a long-range maintenance of the jungle-gym-type structure. Thus, **3** adsorbs H_2O to form $\{[Zn_2(bdc\text{-}(NO_2)_2)_2(dabco)]\cdot 6H_2O\}_n$ (**3**⊃$6H_2O$) without a conversion to a second phase. Considering the results of the H_2O adsorption measurements and XRPD for **1**–**3**, the introduction of NO_2 moieties is effective for enhancing

hydrophilicity and preventing collapse of the regular jungle-gym-type structure. The amounts of NO_2 moiety per dinuclear Zn_2 units are zero (**1**), two (**2**) and four (**3**). As found in H_2O adsorption on compounds **1**–**3**, the different behaviors of framework stability for water coordination is observed; **1**: second phase caused by H_2O coordination at point A, **2**: second phase caused by H_2O coordination between points B and C, **3**: no framework change but adsorb at point D. Considering the results that the infrared spectrum of compound **2** exposed to D_2O vapors shows the lower peaks attributed to NO_2 stretching bands (Fig. S2), the difference would be due to hydrogen bond formations between NO_2 moieties and H_2O molecules, where penetrated H_2O molecules prefer to hydrogen bond to NO_2 moieties rather than coordinate to metal sites.

4. Conclusion

This work demonstrates syntheses and characterization of jungle-gym-type porous coordination polymers containing NO_2 moieties. Selecting NO_2 moiety as hydrogen bonding sites, isomorphous jungle-gym-type structures of **2** and **3** were successfully obtained in which the free NO_2 moieties were oriented to the pores. We used H_2O adsorption measurements and X-ray analysis to demonstrate the pore hydrophilicity in **1**–**3**, revealing that compounds **2** and **3** are rather hydrophilic than **1**. Interestingly, compound **3** adsorbs H_2O in low relative pressure and accommodated six H_2O molecules per pore, and effective hydrogen bonds between NO_2 moieties and H_2O molecules prevented collapse of the framework.

Supplementary material

Crystallographic data for the structural analyses have been deposited with the Cambridge Crystallographic Data Center, CCDC-719046 for complex **2**. Copies of the data can be obtained free of charge from CCDC, 12 Union Road, Cambridge, CB2IEZ, UK. E-mail: deposit@ccdc.cam.ac.uk. Supplementary material associated with this article can be found, in the online version.

Acknowledgments

This work was supported by the Grants-in-Aid for Scientific Research (Young Scientist (B) no. 19750048) and JGC-S Scholarship Foundation.

Appendix A. Supplementary material

Supplementary data associated with this article can be found in the online version at 10.1016/j.jssc.2009.07.048.

References

[1] O.M. Yaghi, M. O'Keeffe, N.W. Ockwig, H.K. Chae, M. Eddaoudi, J. Kim, Nature 423 (2003) 705–714.
[2] S.L. James, Chem. Soc. Rev. 32 (2003) 276–288.
[3] C. Janiak, Dalton Trans. (2003) 2781–2804.
[4] S. Kitagawa, R. Kitaura, S.-i. Noro, Angew. Chem. Int. Ed. 43 (2004) 2334–2375.
[5] G. Férey, C. Mellot-Dranznieks, C. Serre, F. Millange, Acc. Chem. Res. 38 (2005) 217–225.
[6] S. Kitagawa, K. Uemura, Chem. Soc. Rev. 34 (2005) 109–119.
[7] K. Uemura, R. Matsuda, S. Kitagawa, J. Solid State Chem. 178 (2005) 2420–2429.
[8] S. Kitagawa, S.-i. Noro, T. Nakamura, Chem. Commun. (2006) 701–707.
[9] Z. Wang, S.M. Cohen, J. Am. Chem. Soc. 129 (2007) 12368–12369.
[10] Z. Wang, S.M. Cohen, Angew. Chem. Int. Ed. 47 (2008) 4699–4702.
[11] A.D. Burrows, C.G. Frost, M.F. Mahon, C. Richardson, Angew. Chem. Int. Ed. 47 (2008) 8482–8486.
[12] K.K. Tanabe, Z. Wang, S.M. Cohen, J. Am. Chem. Soc. 130 (2008) 8508–8517.
[13] W. Morris, C.J. Doonan, H. Furukawa, R. Banerjee, O.M. Yaghi, J. Am. Chem. Soc. 130 (2008) 12626–12627.
[14] Y. Goto, H. Sato, S. Shinkai, K. Sada, J. Am. Chem. Soc. 130 (2008) 14354–14355.
[15] M. Kondo, T. Okubo, A. Asami, S.-I. Noro, T. Yoshitomi, S. Kitagawa, T. Ishii, H. Matsuzaka, K. Seki, Angew. Chem. Int. Ed. 38 (1999) 140–143.
[16] N.L. Rosi, J. Eckert, M. Eddaoudi, D.T. Vodak, J. Kim, M. O'Keeffe, O.M. Yaghi, Science 300 (2003) 1127–1129.
[17] K. Uemura, A. Maeda, T.K. Maji, P. Kanoo, H. Kita, Eur. J. Inorg. Chem. (2009) 2329–2337.
[18] J.A. Greathouse, M.D. Allendorf, J. Am. Chem. Soc. 128 (2006) 10678–10679.
[19] S.S. Kaye, A. Dailly, O.M. Yaghi, J.R. Long, J. Am. Chem. Soc. 129 (2007) 14176–14177.
[20] D.N. Dybtsev, H. Chun, K. Kim, Angew. Chem. Int. Ed. 43 (2004) 5033–5036.
[21] H. Chun, D.N. Dybtsev, H. Kim, K. Kim, Chem. Eur. J. 11 (2005) 3521–3529.
[22] K. Seki, W. Mori, J. Phys. Chem. B 106 (2002) 1380–1385.
[23] R. Kitaura, F. Iwahori, R. Matsuda, S. Kitagawa, Y. Kubota, M. Takata, T.C. Kobayashi, Inorg. Chem. 43 (2004) 6522–6524.
[24] W. Mori, T. Sato, T. Ohmura, C.N. Kato, T. Takei, J. Solid State Chem. 178 (2005) 2555–2573.
[25] B.-Q. Ma, K.L. Mulfort, J.T. Hupp, Inorg. Chem. 44 (2005) 4912–4914.
[26] B. Chen, S. Ma, F. Zapata, E.B. Lobkovsky, J. Yang, Inorg. Chem. 45 (2006) 5718–5720.
[27] K. Uemura, Y. Yamasaki, Y. Komagawa, K. Tanaka, H. Kita, Angew. Chem. Int. Ed. 46 (2007) 6662–6665.
[28] B. Chen, S. Ma, F. Zapata, F.R. Fronczek, E.B. Lobkovsky, H.-C. Zhou, Inorg. Chem. 46 (2007) 1233–1236.
[29] D.N. Dybtsev, M.P. Yutkin, E.V. Peresypkina, A.V. Virovets, C. Serre, G. Férey, V.P. Fedin, Inorg. Chem. 46 (2007) 6843–6845.
[30] D. Tanaka, M. Higuchi, S. Horike, R. Matsuda, Y. Kinoshita, N. Yanai, S. Kitagawa, Chem. Asian J. 3 (2008) 1343–1349.
[31] K. Li, J.Y. Lee, D.H. Olson, T.J. Emge, W. Bi, M.J. Eibling, J. Li, Chem. Commun. (2008) 6123–6125.
[32] K. Uemura, Y. Komagawa, Y. Yamasaki, H. Kita, Desalination 234 (2008) 1–8.
[33] Z. Wang, K.K. Tanabe, S.M. Cohen, Inorg. Chem. 48 (2009) 296–306.
[34] D.P. Arya, D.J. Jebaratnam, Tetrahedron Lett. 36 (1995) 4369–4372.
[35] T. Higashi, Abscor—Empirical Absorption Correction based on Fourier Series Approximation, Rigaku Corporation, Tokyo, Japan, 1995.
[36] SHELXTL Reference Manual, ver. 5.1, Bruker AXS, Analytical X-ray Systems, Madison, WI, 1997.
[37] A.R. Millward, O.M. Yaghi, J. Am. Chem. Soc. 127 (2005) 17998–17999.
[38] D.J. Tranchemontagne, J.R. Hunt, O.M. Yaghi, Tetrahedron 64 (2008) 8553–8557.
[39] A. Boultif, D.J. Louer, J. Appl. Crystallogr. 24 (1991) 987–993.
[40] The size is measured by considering van der Waals radii for constituting atoms.
[41] T.K. Maji, R. Matsuda, S. Kitagawa, Nature Mater. 6 (2007) 142–148.
[42] Powder samples at points A–D were obtained by interrupting the adsorption measurements, and immediately checked by XRPD.